GeoConvention
Calgary • Canada • March 7-11 2016
OPTIMIZING RESOURCES

A rock-physics based classification of the Doba Basin of Chad

Carl Reine *Canadian Discovery Ltd.*
Chris Szelewski *Retired*
Chaminda Sandanayake *Glencore UK Ltd.*

Summary

Rock-physics models provide the means to translate the elastic properties obtained from seismic inversion, into geological attributes that carry more intuitive meaning for reservoir development. In this presentation, we create a rock model that initially is based on x-ray diffraction (XRD) analysis, fluid analysis, and engineering parameters. We then extend the model to account for the interbedded nature of the reservoir, using net-to-gross ratio (*N*:*G*), along with porosity, to create a geological model of the field.

Introduction

The Mangara field in Chad produces from Lower Cretaceous Sequences of the Doba Basin. The reservoir units consist of interbedded sands and shales of different thicknesses, and the resulting variability in properties makes accurate characterization important for field development.

The approach used in our characterization first involved a quantitative analysis of log data and the calculation of rock-physics models and templates. This analysis established relationships between geological properties of interest, and elastic rock properties that could be obtained from seismic inversion. The results of the rock-property analysis can then be mapped onto the seismic attributes to produce a geologically-classified volume.

Analysis

A statistical analysis of the sand and shale properties observed on the log data was used to identify elastic properties that were significant for reservoir characterization. A large shift is seen between the impedance and v_P:v_S values of sand versus shale points. The porosity of the sands also had an impact on the elastic properties, although to a lesser extent than the lithology. Figure 1 shows the distributions of these elastic values in the reservoir zone.

To incorporate multiple attributes, and to better identify classes of data, crossplots of the elastic attributes were used. Trends of both V_{shale} and porosity are evident on crossplots of P-impedance versus v_P:v_S. These trends are roughly orthogonal, meaning that the two properties may be interpreted with some independence. Yet at the seismic scale, it is unlikely that the thin sand/shale intervals (5-10 m) can be resolved. Figure 2 shows the log data for a well in the field, and the rapidly varying nature of the logs can be seen.

A rock-physics model uses inputs of mineralogy, fluid content, and rock architechture to define the theoretical elastic properties of the assembled parts. With respect to the mineralogy, there is not a continuous transition between sand and shale layers that would involve simply increasing the clay

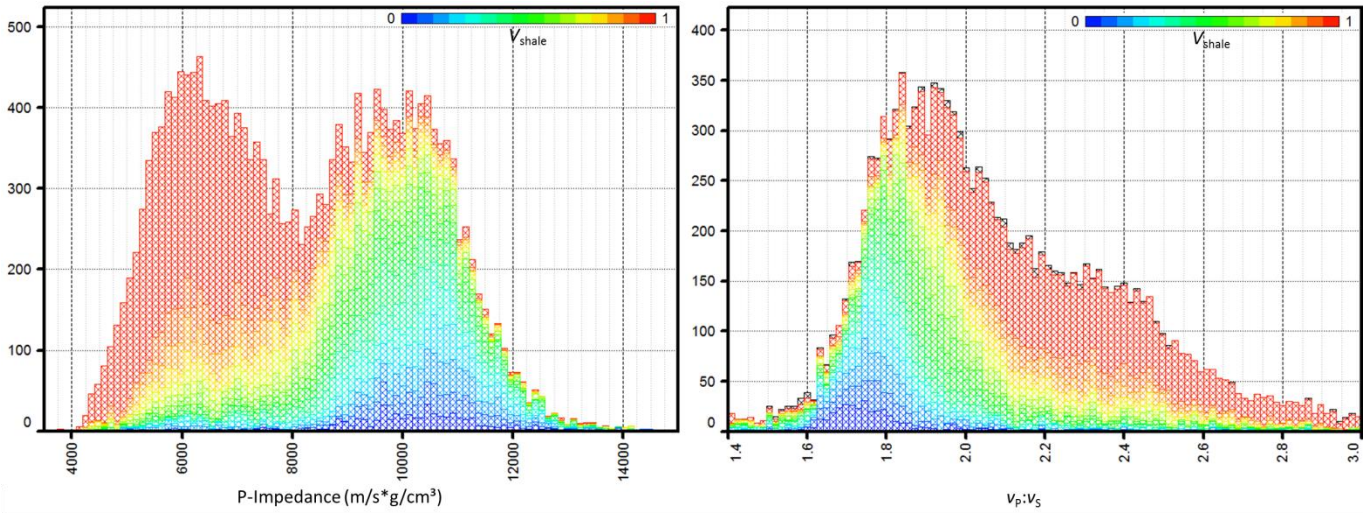

Figure 1. Distributions of P-Impedance and v_P:v_S for the reservoir interval. The data are coloured by V_{shale}, and it is apparent that lithology has a major influence on these two properties.

content of the rock. Rather, the gross reservoir interval is more accurately defined as a binary system of two rock types that occur in different layer thicknesses, and the property of interest in this case is the *N*:*G*.

The sands were first modelled as a five-mineral composition of quartz, potassium feldspar, plagioclase feldspar, kaolinite, and chlorite. The mineral fractions were determined from XRD data, with these five minerals having the highest proportions. Mineral moduli and densities were obtained from Mavko et al. (1998) and Avseth et al. (2005).

The rock was modelled with a fixed amount of cement, which was assumed to be calcite, based on the XRD analysis. To model the dry-frame elastic properties of the rock, a cemented-sand model (Dvorkin and Nur, 1996) was used. The model was calibrated with log measurements of P-wave and S-wave velocity, using a diagenetic trend (Figure 3).

Elastic properties of the saturating hydrocarbons were determined using the relationships of Batzle and Wang (1992), where the reservoir fluids were assumed to be in a single-liquid phase. Fluid analysis established the specific hydrocarbon properties. Finally, the dry-frame rock model was taken to saturated conditions using Gassmann fluid substitution (Mavko et al., 1998).

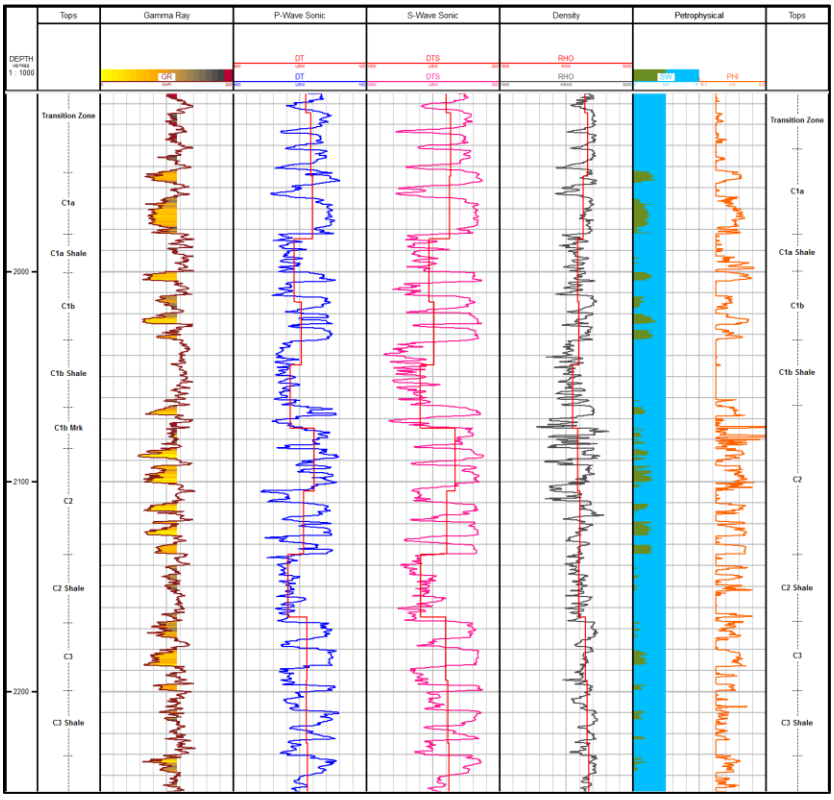

Figure 2. Representative well logs for the field. The gamma-ray log is coloured by V_{shale}, and the effects of lithology on the sonic data can be seen. The red, blocky curves on the sonic and density tracks show the effect of a Backus average with an effective length of 30 m.

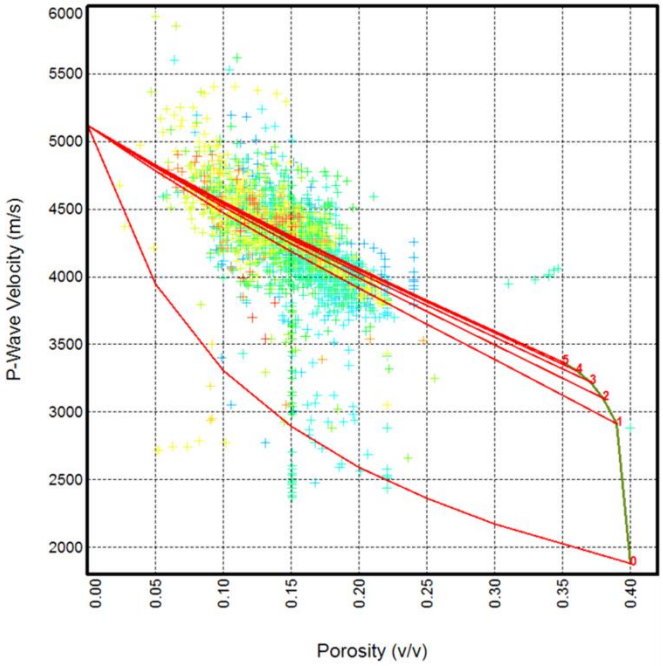

Figure 3. Calibration of the rock-physics model with well values of v_P and porosity. Red lines correspond to percentage of cement in the model, ranging from 0- 5%.

To accommodate a variable *N*:*G*, we followed the methodology outlined by Avseth et al. (2009). The shale properties were taken from log data where V_{shale} = 1. With sand properties modelled for a range of porosities, variable *N*:*G* were then modelled by performing a Backus average (Backus, 1962) of the two lithologies. This averaging was done at each porosity value, for *N*:*G* values from 0% to 100%.

Figure 4 shows a rock-physics template with the well data for calibration. Lines of constant *N*:*G* and porosity are displayed, and both the shale and porosity trends seen in the well data follow the lines of the template. This provides confidence in the predictive ability of the rock-physics model, which was then used to guide the crossplot interpretation of the seismic attributes obtained through AVO inversion.

Seismic classification in the zone of interest followed the trends defining low, medium, and high *N*:*G*. The highest *N*:*G* points were further divided into low-, medium-, and high-porosity classes (Figure 5).

Conclusions

Well analysis was carried out to determine how the elastic behaviour of the logs was distinguished by rock properties, and a theoretical rock-physics model was created to assist in this distinction. This analysis was the basis for assigning geological classes to groups of seismic attributes. The subdivision of the reservoirs was based on both *N*:*G* and porosity. The resulting lithology volume proved to be a good indicator of net reservoir, showing variations in continuity and thickness that were confirmed by additional drilling. The classified volume was used to produce sand probability maps that could be input into a reservoir model.

Acknowldegements

The authors would like to thank Glencore, the Ministère de l'Energie et du Pétrole (Chad), and the Société des Hydrocarbures du Tchad for their permissions to publish this work.

References

Avseth, P., T. Mukerji, and G. Mavko, 2005, Quantitative seismic interpretation: Applying rock physics tools to reduce interpretation risk: Cambridge University Press.

Avseth, P., A. Jorstad, A.-J. van Wijngaarden, and G. Mavko, 2009, Rock physics estimation of cement volume, sorting, and net-to-gross in North Sea sandstones: The Leading Edge, **28**, 98-108.

Backus, G.E., 1962, Long-wave elastic anisotropy produced by horizontal layering: Journal of Geophysical Research, **67**, 4427-4440.

Batzle, M., and Z. Wang, 1992, Seismic properties of pore fluids: Geophysics, **57**, 1396-1408.

Dvorkin, J., and A. Nur, 1996, Elasticity of high-porosity sandstones: Theory for two North Sea data sets: Geophysics, **61**, 1363-1370.

Mavko, G., T. Mukerji, and J. Dvorkin, 1998, The rock physics handbook: Tools for seismic analysis in porous media: Cambridge University Press.

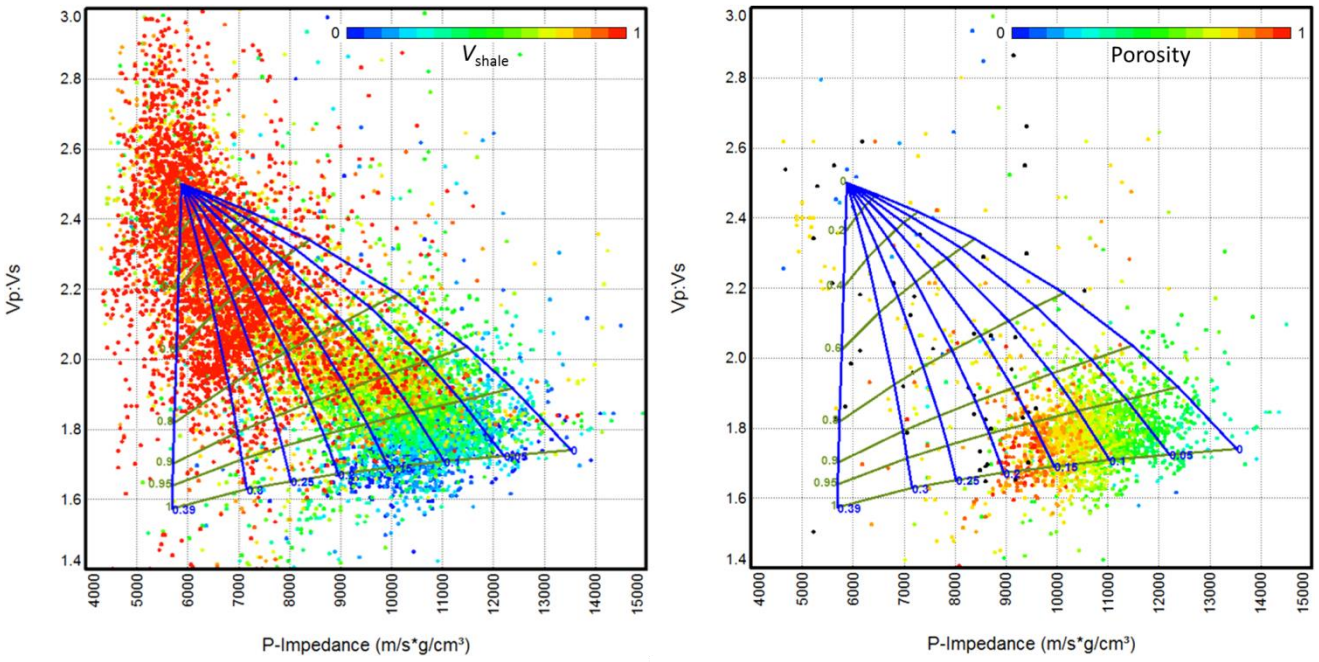

Figure 4. Rock-physics templates in the v_P:v_S versus P-impedance domain. Blue lines connect points of constant porosity, and green lines connect points of constant *N*:*G*. There is good correspondence with the V_{shale} and porosity trends observed on well data.

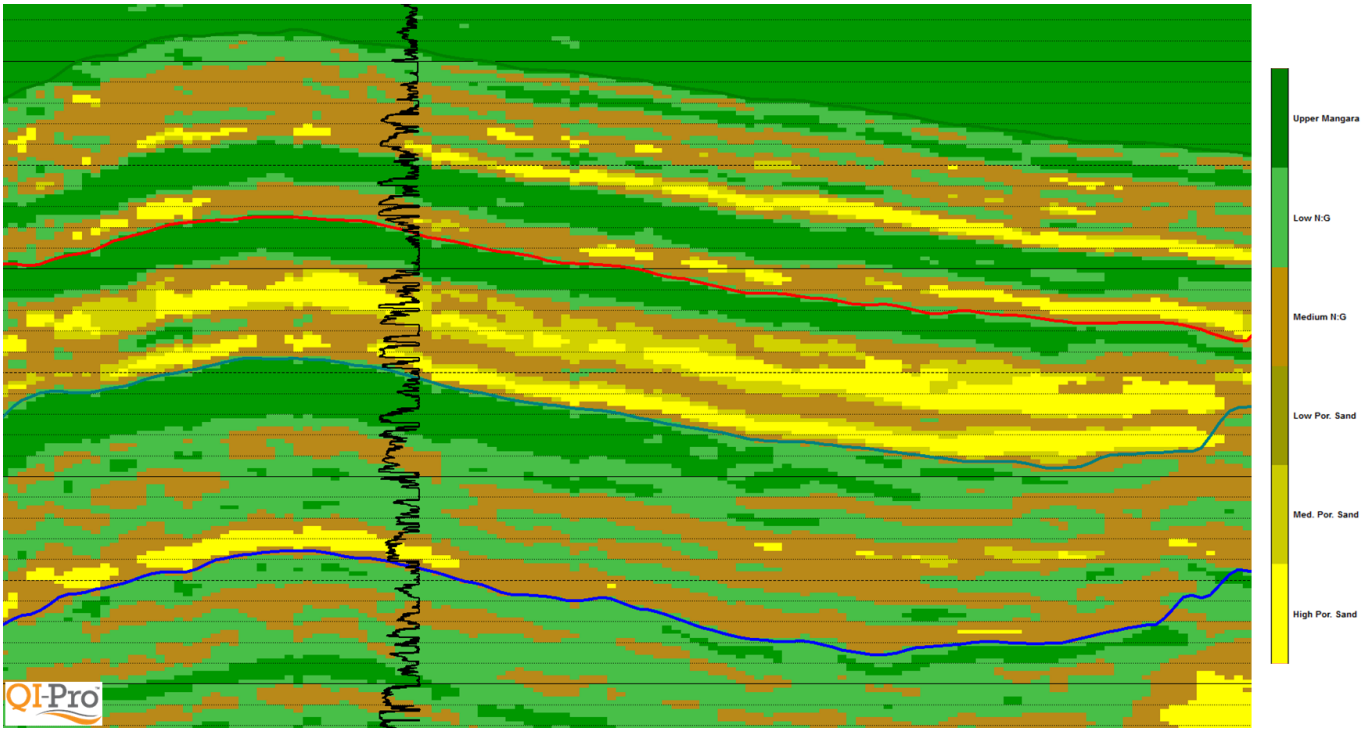

Figure 5. Classified seismic section showing areas of shale/low *N*:*G* (green), medium *N*:*G* (brown), and high *N*:*G* sands (yellow). A V_{shale} log is shown for correlation purposes.